# Reorganization of Lipid Domain Structure in Membranes by a Transmembrane Peptide: An ESR Spin Label Study on the Effect of the *Escherichia coli* Outer Membrane Protein A Signal Peptide on the Fluid Lipid Domain Connectivity in Binary Mixtures of Dimyristoyl Phosphatidylcholine and Distearoyl Phosphatidylcholine

M. B. Sankaram,* D. Marsh,‡ L. M. Gierasch,§ and T. E. Thompson*

*Department of Biochemistry, University of Virginia Health Sciences Center, Charlottesville, Virginia 22908 USA; ‡Abteilung Spektroskopie, Max-Planck-Institut für biophysikalische Chemie, D-37077 Göttingen, Germany; and §Departments of Biochemistry and Pharmacology, University of Texas Southwestern Medical Center, Dallas, Texas 75235-9071 USA

ABSTRACT The effect of a transmembrane peptide on the domain structure of a two-component, two-phase lipid bilayer composed of dimyristoyl phosphatidylcholine (DMPC) and distearoyl phosphatidylcholine (DSPC) was examined by spin label electron spin resonance (ESR) spectroscopy. The peptide, pOmpA, is the hydrophobic, 25-residue signal sequence of the outer membrane protein A from *Escherichia coli*. Nitroxide derivatives of the phospholipid DSPC, 16-DSPCSL, and of the pOmpA signal peptide, pOmpA-IASL, were used as probes. The first-derivative lineshapes of the ESR spectra were analyzed using a normalized intensity ratio, $R$, that gives information on the average sizes of the disconnected fluid domains and their point of connectivity (Sankaram, M. B., D. Marsh, and T. E. Thompson. 1992. *Biophys. J.* 63:340–349). In the absence of the peptide, the number of fluid lipid domains does not vary with the fraction of lipid that is in the fluid phase, and phase conversion is accomplished solely by changes in the domain size. The phase boundaries of the lipid mixture remain largely unchanged by the presence of the peptide at mole fractions up to 0.02, but both the size and number of the fluid domains is changed, and the point at which they become connected is shifted to lower fractions of the fluid phase. In addition, the number of domains in the presence of the peptide no longer remains constant but increases from a domain density at low fractions of the fluid phase that is much lower than that in the absence of peptide to one that is comparable to the natural state in the absence of peptide at the point of domain connectivity. A simple model is presented for the process of domain fission, where the latter is determined by a balance between the effects of peptide concentration in the fluid domains, the line tension at the domain boundaries, and the distributional entropy of the domains.

## INTRODUCTION

The detection, quantitation, and examination of the physiological significance of in-plane lipid domains in model and biological membranes is a subject of intensive recent study (Bultmann et al., 1991; Edidin, 1990; Melo et al., 1992; Sankaram et al., 1992; Vaz et al., 1989, 1990; Vaz, 1992; Thompson et al., 1992). Domains in biological membranes, which contain both protein and lipid molecules, can be detected directly by fluorescence microscopic methods (Edidin, 1990), whereas detection of domains in lipid bilayers is usually based on fluorescence photobleaching studies (Vaz et al., 1989, 1990; Vaz, 1992; Jovin and Vaz, 1989).

Recently, we have proposed a method that could be suitable for analyzing spin-spin interactions between nitroxide spin labels that are spatially separated from one another when they are distributed statistically among disconnected lipid domains (Sankaram et al., 1992). The novelty of this method lies in the fact that it utilizes an internally normalized intensity ratio parameter measured on symmetric, first-derivative electron spin resonance (ESR) spectral lines (Bales, 1980, 1982, 1989). The intensity ratio, $R$, is defined as $V'/2V^{pp}$, where $V^{pp}$ is the maximum peak-to-peak intensity and $V'$ is the intensity at a position in the wings of a first-derivative ESR line that is a constant multiple of the peak-to-peak linewidth (see Fig. 1). This intensity ratio, $R$, is a property only of the lineshape and is independent of the size of the spectral broadening (e.g., from Lorentzian linebroadening mechanisms such as those caused by oxygen, slow exchange, or rapid rotational diffusion). In this study (Sankaram et al., 1992) it was shown by spectral simulations

that $R \leq R^L$ for homogeneously distributed spin labels, where $R^L$ is the intensity ratio of a Lorentzian lineshape. The condition $R > R^L$ was shown to hold when the spin labels are distributed statistically into disconnected domains, and the exchange of the labels between the domains is slow on the time-scale of the ESR experiment. Further, the spectral simulations showed that the ratio $R$ increases with increasing occupancy of the domains by spin labels up to a certain density, beyond which it decays to $R^L$ (Sankaram et al., 1992).

Under certain circumstances and with certain assumptions (that are given later), the average size of disconnected fluid and gel domains could be estimated using this method. This was done from measurements of $R$ in the ESR spectra of a spin-labeled derivative of dimyristoyl phosphatidylcholine (DMPC) with the nitroxide group at the 13 position in the sn-2 acyl chain, 13-DMPCSL, incorporated into two-component, two-phase lipid bilayers formed from DMPC and distearoyl phosphatidylcholine (DSPC) (Sankaram et al., 1992). The method does not provide information on a possible heterogeneity in domain sizes, but only yields the effective sizes averaged over the distribution of domains. Nevertheless, the data were found to be consistent with a model in which an increase in the proportion of a given phase (fluid or gel) results in an increase in the size of the disconnected domains of that phase, with no change in the number of domains. In this paper, we report results obtained (a) on the DMPC/DSPC system with a spin-labeled derivative of DSPC containing the nitroxide moiety at the 16 position in the sn-2 acyl chain and (b) on the DMPC/DSPC system with an iodoacetamide-spin-labeled 25-residue transmembrane, hydrophobic peptide, pOmpA-IASL, and (c) with DMPC/DSPC mixtures containing the unlabeled peptide, pOmpA (Sankaram et al., 1993), and spin-labeled derivatives of DMPC or of DSPC. The peptide corresponds to the N-terminal signal peptide plus the first four residues of the outer membrane protein A from Escherichia coli, and has a primary sequence MKKTAIAIAVALAGTATVA-QAAPKD.

## MATERIALS AND METHODS

### Materials

The phospholipids, dimyristoyl phosphatidylcholine, DMPC, and distearoyl phosphatidylcholine, DSPC, were from Avanti Chemical Co. (Alabaster, AL). The iodoacetamide spin label, N-[4-(iodoacetyl)amino]-2,2,6,6-tetramethylpiperidinyl-N-oxyl, IASL, was from Molecular Probes Inc. (Eugene, OR). 16-SASL was from Sigma Chemical Co. (St. Louis, MO).

### Methods

#### Synthesis of 13-DMPCSL and 16-DSPCSL

The lipid spin labels, 13-DMPCSL and 16-DSPCSL, were synthesized by acylation of 1-myristoyl phosphatidylcholine and 1-stearoyl phosphatidyl-choline with 13-MASL and 16-SASL, respectively, using methods described previously (Marsh and Watts, 1982).

### Synthesis of pOmpA

The peptide pOmpA was synthesized by standard methodology using N-terminal, tert-butyloxycarbonyl (t-boc)-protected amino acids on an ABI 430A automated synthesizer. The peptide was deprotected and cleaved from the resin using anhydrous hydrofluoric acid. Purification of the peptide was carried out by high pressure liquid chromatography on a Vydac C4 column eluted with acetonitrile/water gradients containing 0.1% trifluoroacetic acid. Amino acid content and sequence were verified by quantitative amino acid analysis and peptide sequencing.

### Synthesis of pOmpA-IASL

The spin-labeled peptide, pOmpA-IASL, was prepared according to published methods (Griffith and McConnell, 1966). Briefly, 200 μmol of IASL was added to 200 μmol of the pOmpA peptide in a pH 11 Tris buffer (10 mM Tris, 10 mM NaCl) at 0°C. The solution was stirred overnight at 0°C. The reaction mixture was purified by preparative liquid chromatography on a Vydac C18 column eluted with acetonitrile/water gradients containing 0.1 mol% trifluoroacetic acid. Two spin-labeled peptide fractions were isolated from the column. The ratio of spin label to peptide in the major spin-labeled peptide fraction was determined to be 0.95 by assaying the samples for peptide content (Lowry et al., 1951) and for spin label content (Sachse et al., 1987). The ratio of spin label to peptide in the minor spin-labeled peptide fraction, with a longer retention time, was determined to be 1.7. The major component was used for the ESR experiments described in this paper. The high spin label to peptide ratio of the minor component suggests that this fraction contains pOmpA with more than one site spin-labeled. It is also likely that there are several unresolved spin-labeled pOmpA positional isomers in this fraction.

The site of spin labeling for the major component isolated by liquid chromatography was determined by gas chromatography-mass spectrometry on enzymatically derived dipeptides of the spin-labeled pOmpA (Krutzsch and Pisano, 1977; Krutzsch, 1983). Briefly, the method involves digestion of pOmpA-IASL by dipeptidyl aminopeptidase to produce dipeptides starting from the amino terminus, trimethylsilylation of the resulting dipeptides for gas chromatographic analysis, and identification of the structure of the derivatized dipeptides by mass spectrometry. The gas chromatographic analysis of pOmpA and pOmpA-IASL showed differences in elution only for the N-terminal M-K dipeptide, suggesting that iodoacetamide was covalently linked either to the free amino terminus, to the side chain of methionine, or to the side chain of lysine. A preliminary analysis of the mass spectrometry data on the M-K dipeptide showed that IASL is covalently attached to the side chain of methionine (M. B. Sankaram, unpublished observations).

### Preparation of lipid-peptide complexes

The pOmpA-IASL peptide was incorporated into DMPC/DSPC (50:50 mol/mol) and DMPC/DSPC (40:60 mol/mol) vesicles as described (Sankaram et al., 1993). A 1 mg/ml solution of the pOmpA peptide was prepared in water, and the pH was adjusted to 2.5. Desired aliquots from this stock solution were added to aqueous dispersions of large unilamellar lipid vesicles. Large unilamellar vesicles were prepared by the method of extrusion. The complexes were dialyzed against a Tris buffer (5 mM Tris, pH 7.3). The lipid-peptide complexes were then repeatedly freeze-thawed to produce multilamellar vesicles. This procedure was necessary to produce a homogeneous system with the peptide distributed equally throughout the system (Sankaram et al., 1993). Peptide and lipid concentrations of the lipid-peptide complexes were assayed by the methods of Lowry et al. (1951) and Eibl and Lands (1969), respectively.

### ESR spectroscopy

For the ESR experiments, multilamellar vesicles were prepared from mixtures of DMPC and DSPC. The samples contained either 50:50 (mol/mol) or 40:60 (mol/mol) mixtures of the phospholipids. For each lipid composition, one set of samples was prepared with the phospholipid spin label,

16-DSPCSL, at different concentrations in the range 0.1–3 mol%. A second set of samples contained the peptide spin label, pOmpA-IASL, in the same spin label concentration range. A third set of samples contained 2 mol% unlabeled peptide, pOmpA, and the phospholipid spin labels, 13-DMPCSL or 16-DSPCSL (0.1–3 mol% spin label). For each sample, ESR spectra were recorded in the temperature range 0–70°C. In this temperature range, the DMPC/DSPC mixed bilayers undergo a thermotropic phase transition from a mixed gel phase, through a gel-fluid coexistence region to a fluid phase (Knoll et al., 1981). ESR spectra were recorded on a Varian E-line 9 GHz spectrometer. The details of instrumentation and data processing are given in Sankaram and Thompson (1990) and in Sankaram et al. (1992), respectively.

## RESULTS

### ESR spectra of phospholipid and peptide spin labels in DMPC/DSPC mixtures

Representative ESR spectra of the phospholipid spin label, 16-DSPCSL, and of the peptide spin label, pOmpA-IASL, in 50:50 DMPC/DSPC (mol/mol) mixtures are shown in Fig. 2. With increasing temperature, the spectra of both spin labels exhibit motional narrowing that is manifest as a decrease in linewidth of the three hyperfine lines. At any given temperature, the spectra of the peptide spin label, pOmpA-IASL, are sharper than those of the phospholipid spin label, 16-DSPCSL. This result is most likely due to the presence of the nitroxide moiety of 16-DSPCSL in the hydrophobic core of the lipid bilayer, whereas the nitroxide-derivatized N-terminal residue is located near the lipid-water interface. Despite this difference in the location of the spin label in 16-DSPCSL and pOmpA-IASL, the ESR spectra of both labels are sensitive to the thermotropic phase changes of the host lipid bilayer.

### Peak-to-peak linewidth

The dependence on temperature of the apparent peak-to-peak linewidth, $\Delta H^{pp}$, of the high-field hyperfine line in the ESR spectra of 16-DSPCSL and of pOmpA-IASL in an equimolar mixture of DMPC and DSPC is shown in Fig. 3. In both cases, the temperature dependence of $\Delta H^{pp}$ exhibits discon-
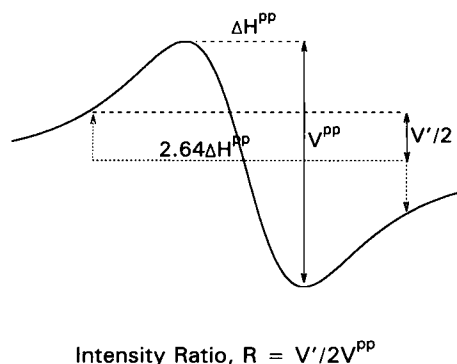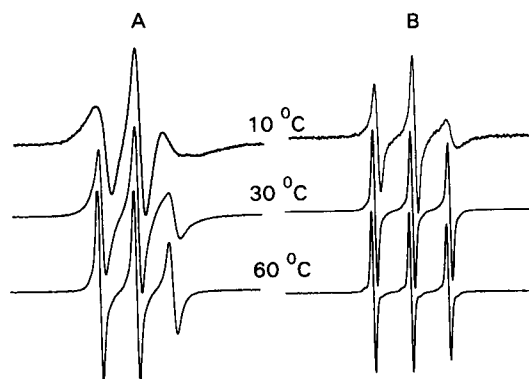


FIGURE 2   ESR spectra in DMPC/DSPC 50:50 (mol/mol) mixtures of (A) 16-DSPCSL and of (B) pOmpA-IASL. The spin label concentration in both cases is 1 mol%. According to the temperature-composition phase diagram of Knoll et al. (1981), the DMPC/DSPC system undergoes a thermotropic phase transition from a mixed gel phase at 10°C through a gel-fluid coexistence region at 30°C to a fluid phase at 60°C.



FIGURE 1   Definition of the peak-to-peak linewidth, $\Delta H^{pp}$, and of the intensity ratio, $R$, of a first-derivative display of an electron spin resonance spectral line. See text and Sankaram et al. (1992), Bales (1980, 1982, 1989) for further details of the intensity ratio.

tinuities at three characteristic temperatures shown as vertical dotted lines in each panel. For pOmpA-IASL (Fig. 3 B), the high temperature discontinuity is only evident on a plot with expanded vertical scale (for which the other discontinuities also become clearer). In Fig. 4, the data in Fig. 3, A and B are plotted on an expanded scale along with the temperature dependence of the linewidths measured for 16-DSPCSL in the DMPC-DSPC-pOmpA system. The three characteristic temperatures are identified empirically as described before (Sankaram et al., 1992). The first discontinuity occurs when, at the solidus, the system undergoes a transition from a mixed gel phase region to a gel-fluid coexistence region. The second discontinuity is observed at the fluidus at which the gel-fluid coexistence ceases to exist and the system is in a single fluid phase. As more clearly seen in Fig. 4, at intermediate temperatures between the solidus and the fluidus, the third discontinuity is seen that corresponds to the point of connectivity. The point of connectivity is the temperature below which the fluid phase is disconnected to form isolated fluid lipid domains dispersed in a continuous, reticular gel phase (Vaz et al., 1989). Above the point of connectivity, the complementary situation is obtained namely, the gel phase forms the disconnected domains in a continuous fluid phase (Vaz et al., 1989). Because the domain connection is a relatively long range effect, the point of connectivity is defined by the point at which the abrupt drop in linewidth begins (cf. Fig. 4), rather than by some mid-point position. These relationships were established for the pure lipid system by comparison with the phase diagram and points of connectivity obtained from FRAP measurements (Sankaram et al., 1992; Vaz et al., 1989) and are generalized here to the peptide-containing system.

As seen in Fig. 3 for the DMPC/DSPC 50:50 (mol/mol) mixtures, the first and the second discontinuity at the solidus and the fluidus, respectively, occur at the same temperature for both 16-DSPCSL and pOmpA-IASL. Also, in experiments with DMPC/DSPC 40:60 (mol/mol) mixtures

FIGURE 3 Dependence on temperature of the apparent peak-to-peak linewidth ($\Delta H^{pp}$) of the high-field hyperfine line in the ESR spectra of (A) 16-DSPCSL and (B) pOmpA-IASL in DMPC/DSPC 50:50 (mol/mol) bilayers. The spin label concentration was 2 mol%. The full lines are a third order polynomial fit to the gel phase data and linear regression for the fluid phase data. The extrapolated values of the linewidth for the gel and fluid phases were obtained by this fitting procedure and are indicated by the dashed lines. The vertical dotted lines indicate the solidus and fluidus phase boundaries determined from the temperature-composition phase diagram (Sankaram et al., 1992; Knoll et al., 1981) and the point of connectivity taken as the temperature at which a sudden drop in $\Delta H^{pp}$ begins (Sankaram et al., 1992).
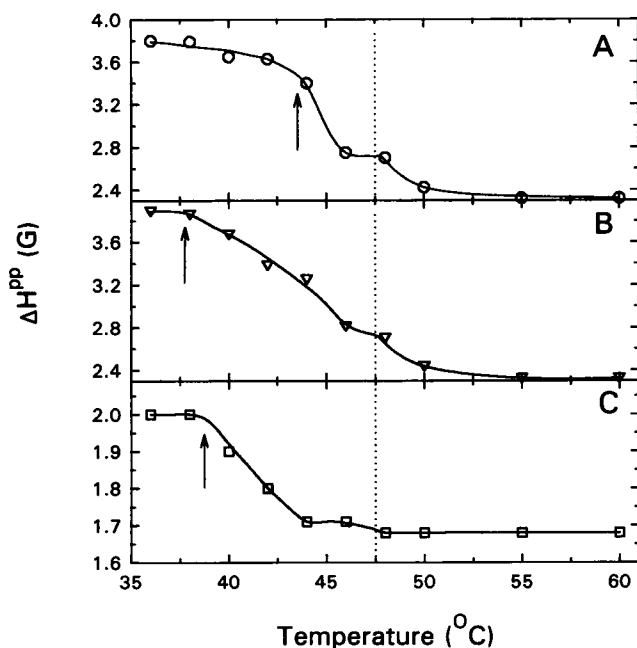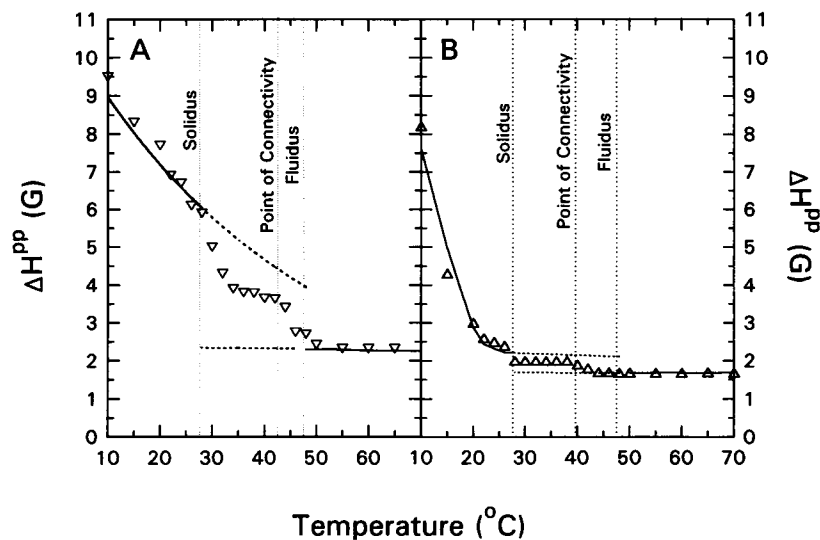
FIGURE 4 Dependence on temperature of the apparent peak-to-peak linewidth ($\Delta H^{pp}$) of the high-field hyperfine line in the ESR spectra of (A)16-DMPCSL in DMPC/DSPC 50:50 (mol/mol) bilayers, (B) 16-DSPCSL in DMPC/DSPC 50:50 (mol/mol) bilayers containing 2 mol% pOmpA, and (C) pOmpA-IASL in DMPC/DSPC 50:50 (mol/mol) bilayers. The spin label concentration was 2 mol%. The full lines are drawn for visual guidance. The vertical dotted line indicates the fluidus phase boundary determined from the temperature-composition phase diagram (Knoll et al., 1981). The arrows indicate the point of connectivity taken as the temperature at which a sudden drop in $\Delta H^{pp}$ begins (Sankaram et al., 1992). The vertical scale is expanded relative to that in Fig. 3.

(Sankaram et al., 1992), to within the experimental accuracy, the temperature discontinuity at the solidus does not depend on whether the system contains the phospholipid spin labels, the peptide spin label or a low concentration of unlabeled peptide, pOmpA, along with either 13-DMPCSL or 16-DSPCSL (data not shown).

However, the point of connectivity measured with pOmpA-IASL occurs at a lower temperature than that measured with 16-DSPCSL (see Fig. 4). The point of connectivity measured with the phospholipid spin labels for the DMPC/DSPC mixed bilayers containing 2 mol% unlabeled peptide, OmpA, occurs at a slightly lower temperature than that measured with the peptide label, pOmpA-IASL, for DMPC/DSPC mixtures (see Table 1).

## Intensity ratio

The dependence on spin label concentration of the observed intensity ratio, $R_{obs}$, of the middle hyperfine line in the ESR spectra of 16-DSPCSL is shown in Fig. 5. The spin label was present in either 50:50 (mol/mol) mixtures (Fig. 5 A) or in 40:60 (mol/mol) mixtures (Fig. 5 B) of DMPC and DSPC. Two important observations are made from the data shown in Fig. 5. First, the intensity ratio $R_{obs}$ in the gel-fluid coexistence region is greater than $R^L$ (=0.213, the limiting intensity ratio for a Lorentzian lineshape), at all concentrations of 16-DSPCSL and at all temperatures. Second, at any given temperature in the gel-fluid coexistence region, $R_{obs}$ is seen in Fig. 5 first to increase with increasing concentration of 16-DSPCSL and then to decrease. The observations that $R_{obs} > R^L$ and that $R_{obs}$ goes through a maximum, as is predicted by simulations, strongly suggest the presence of disconnected fluid lipid domains at the temperatures for which the $R_{obs}$ data are shown in Fig. 5 (Sankaram et al., 1992). It will be noted that other effects, namely the coexistence of two-component spectra and the presence of spectral anisotropy, potentially may give rise to values of $R_{obs} > R^L$. However, neither of these is likely to give rise to the characteristic dependence of $R_{obs}$ on spin label concentration that is demonstrated in Fig. 5. Additionally, for fractional differences in linewidth of <0.1, to which the subsequent analysis is restricted, two-component spectra alone do not yield values of $R_{obs} > R^L$ (see Fig. 4 A of Sankaram et al., 1992).

In Fig. 6, the dependence on spin label concentration of $R_{obs}$ of the middle hyperfine line in the ESR spectrum of

**TABLE 1   Point of connectivity in DMPC/DSPC lipid mixtures measured by FRAP using the fluorescent probe NBD-POPE and by ESR using nitroxide spin labels, 13-DMPCSL and 16-DSPCSL**

| System | Probe | Point of connectivity (°C) | Fluid fraction at point of connectivity | Technique | Reference |
|---|---|---|---|---|---|
| DMPC/DSPC | NBD-POPE | 42 | 0.59 | FRAP | Vaz et al., 1989 |
| DMPC/DSPC | 13-DMPCSL | 42.2 ± 1.4 | 0.61 ± 0.09 | ESR | Sankaram et al., 1992 |
| DMPC/DSPC | 16-DSPCSL | 41.5 ± 1.5 | 0.57 ± 0.07 | ESR | Fig. 4 A |
| DMPC/DSPC | pOmpA-IASL | 39.6 ± 1.3 | 0.49 ± 0.05 | ESR | Fig. 4 B |
| DMPC/DSPC/pOmpA | 13-DMPCSL | 38.7 ± 1.5 | 0.46 ± 0.05 | ESR | This work, data not shown |
| DMPC/DSPC/pOmpA | 16-DSPCSL | 38.2 ± 1.5 | 0.44 ± 0.04 | ESR | Fig. 4 C |

The concentration of the spin labels, 13-DMPCSL, 16-DSPCSL, pOmpA-IASL, and of the peptide, pOmpA were 2 mol%.

FIGURE 5   Dependence on the concentration of 16-DSPCSL of the intensity ratio, $R_{obs}$, of the middle hyperfine line in the ESR spectrum of 16-DSPCSL. Data were obtained from (A) 50:50 (mol/mol) mixtures of DMPC/DSPC and (B) 40:60 (mol/mol) mixtures of DMPC/DSPC. In A the temperatures are 32°C (O), 34°C (●), and 38°C (▽), and in B, they are 34°C (O), 38°C (●), and 42°C (▽). The dashed line in both A and B is the maximum value for the intensity ratio, $R^L = 0.213$, for a Lorentzian line (Sankaram et al., 1992).
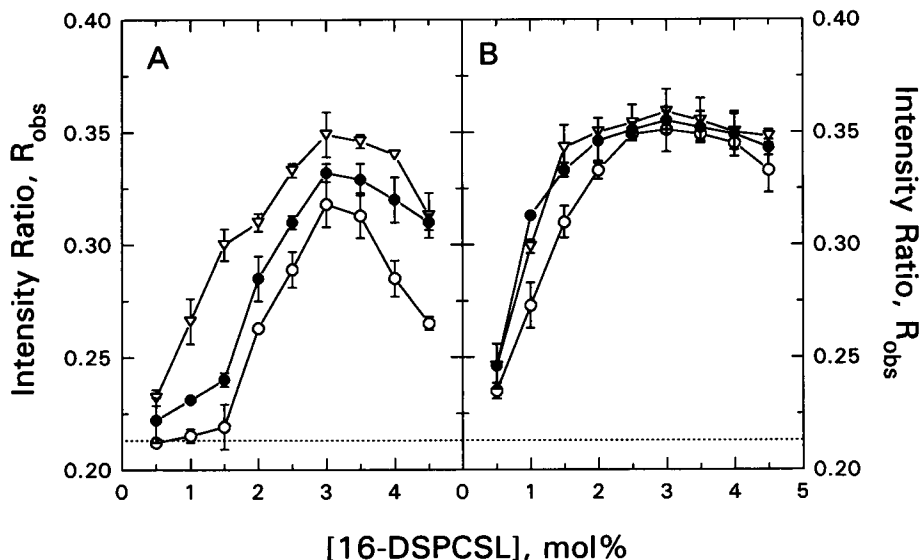


pOmpA-IASL is shown for the 40:60 (mol/mol) and 50:50 (mol/mol) mixtures of DMPC and DSPC. Similar to the data shown in Fig. 5 for the lipid spin label, 16-DSPCSL, the data for the peptide spin label, pOmpA-IASL, show that (a) in the gel-fluid coexistence region, $R_{obs}$ is greater than $R^L$ and (b) $R_{obs}$ goes through a maximum when plotted as a function of the concentration of pOmpA-IASL. As before, these results suggest that pOmpA-IASL is distributed in disconnected domains in the gel-fluid coexistence region (Sankaram et al., 1992).

## Average number of spin labels per disconnected fluid domain, $N_f$

From the intensity ratio measurements, the average number of spin-labeled lipids per disconnected fluid domain, $N_f$, was estimated using the method proposed previously (Sankaram et al., 1992). Assuming that there is only slow exchange of the spin labels between phases, the intensity ratio observed, $R_{obs}$, is weighted by the intensity ratio contributions from the gel and the fluid phase components. Estimates of likely exchange rates indicate that these would be insufficiently fast to provide averaging of spectral components with linewidth differences of 1 G or more, even if this were close to the level

found in fluid bilayers. It has previously been shown that when the fractional change in the peak-to-peak linewidth between the gel and fluid phase spectra is less than 0.1, the observed intensity ratio, $R_{obs}$ is approximated reasonably well by a weighted-average of the component $R$ values (Eq. 5 of Sankaram et al., 1992). As in the previous work (Sankaram et al., 1992), only data for the *central* line that meet this criterion are used in the analysis. When the fluid phase is disconnected, $R_{obs}$ is given by

$$R_{obs} = fR_f + (1 - f)R_g, \tag{1}$$

where $R_f$ and $R_g$ are the intensity ratios of the fluid and the gel phase component spectra, respectively, and $f$ is the mole fraction of the spin label in the fluid phase. Because the gel phase is the continuous phase, $R_g$ can be assumed to be always a constant that is either equal to the limiting value of 0.213 for a Lorentzian line or can be obtained by extrapolation of the intensity ratios in the gel phase (Sankaram et al., 1992). The mole fraction of the lipid spin labels, 13-DMPCSL or 16-DSPCSL, in the fluid phase, $f$, can be assumed to be the mole fraction of their respective parent lipids, DMPC and DSPC, in the fluid phase (Sankaram et al., 1992). This parameter is easily obtained from the

FIGURE 6 Dependence on the concentration of the spin-labeled peptide, pOmpA-IASL, of the intensity ratio, $R_{obs}$, of the middle hyperfine line in the ESR spectrum of pOmpA-IASL. Data were obtained from (A) 50:50 (mol/mol) mixtures of DMPC/DSPC and (B) 40:60 (mol/mol) mixtures of DMPC/DSPC. In A, the temperatures are 32°C (O), 34°C (●), and 38°C (∇), and in B, they are 34°C (O), 38°C (●), and 42°C (∇). The dashed line in both A and B is the maximum value for the intensity ratio, $R^L = 0.213$, for a Lorentzian line (Sankaram et al., 1992).
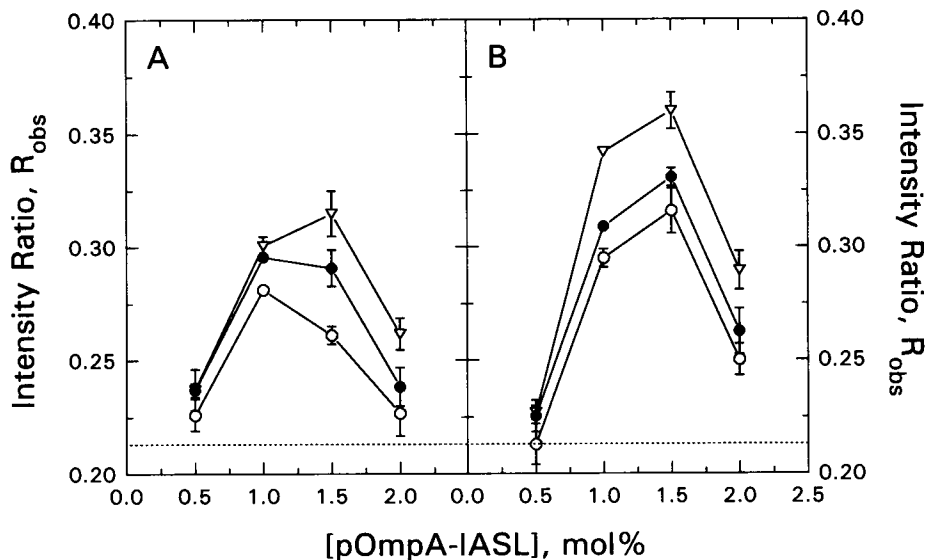


temperature-composition phase diagram (Knoll et al., 1981). The peptide, pOmpA, and the peptide spin label, pOmpA-IASL, are assumed to be localized entirely in the fluid phase. No direct experimental data on the partitioning of the peptide are available, but it is likely from general considerations of free volume and packing that the peptide partitions strongly into the fluid phase. Therefore, it is taken that $f = 1$ for the peptide of either form. This assumption is unlikely to influence the general conclusions reached, although the exact quantitative results will be affected.

The relation between $R_f$, obtained from Eq. 1, and the average number of the spin labels per disconnected fluid domain, $N_f$, has been calculations for a statistical distribution of spin labels in Sankaram et al. (1992). At low occupancy of disconnected domains by spin labels, $R_f$ increases with $N_f$, but decreases nearly exponentially when $N_f$ is greater than about 8 (Sankaram et al., 1992). The calibration curve given in Sankaram et al. (1992) was used to determine $N_f$ from $R_f$. In the exponential region for $N > 8$, the dependence of $R$ on $N$ for fluid or gel domains is given to a good approximation by

$$R = 0.40293 \exp(-0.16344N) + 0.213. \qquad (2)$$

Experimental data points only in this region where $N_f > 8$ were used to determine the values of $N_f$. This is because, at lower values of $N$, the calibrations are sensitive to various complicating factors, such as the individual linewidths, degree of Gaussian inhomogeneous broadening, and most probably also to heterogeneity in domain size (Sankaram et al., 1992), whereas for $N > 8$ this is not the case. These latter values of $N_f$ will be used in the following discussion to give information on the disconnected fluid domain structure in the presence and absence of the peptide. In this work, only the disconnected fluid domains that are present between the solidus and the point of connectivity will be considered. This is because the difference in linewidths of the ESR spec-

tra of the 16-DSPCSL and of the pOmpA-IASL in the fluid and gel phases does not fulfill the criterion for the validity of Eq. 1 (cf. above) in the region between the point of connectivity and the fluidus.

## DISCUSSION

### Effect of pOmpA on phase behavior

In the peptide concentration range 0–3 mol% used in this study, the temperature at which a conversion of the DMPC/DSPC system from a mixed gel region to a gel-fluid coexistence region takes place (solidus) and the temperature at which the system goes from the gel-fluid coexistence region to a single fluid phase (fluidus) are not affected appreciably either by the presence of the phospholipid spin labels (13-DMPCSL and 16-DSPCSL), the presence of the peptide spin label (pOmpA-IASL), or when the unlabeled peptide, pOmpA, is incorporated into the mixed bilayers along with either phospholipid spin label (see Figs. 3 and 4 and Sankaram et al., 1992). This result suggests that, to within the experimental accuracy, inclusion of the peptide in disconnected fluid domains in this concentration range does not alter the phase behavior of DMPC/DSPC mixtures. Also, the proportion of the gel phase as detected by $^2H$ NMR measurements (Sankaram and Thompson, 1992) is the same for the DMPC–DSPC system as for the DMPC-DSPC-pOmpA system at four pOmpA concentrations in the range 1–4 mol% (M. B. Sankaram and T. E. Thompson, unpublished observations).

### Effect of pOmpA on the point of connectivity

As seen from Figs. 3 and 4 and Table 1, although the phase boundaries are relatively unaffected by the peptide, the peptide does decrease markedly the fraction of fluid phase at which the domains become connected. In the absence of the

peptide, the point of connectivity determined from the temperature dependence of the linewidths of the spin-labeled lipids occurs at a fluid fraction (obtained using the lever rule) of $F = 0.57$–$0.61$, in good agreement with the value of $F = 0.59$ determined by FRAP experiments on the same system (Vaz et al., 1989). In the presence of the peptide, however, the point of connectivity for the DMPC/DSPC 50:50 (mol/mol) mixture occurs at a lower temperature and, hence, at a lower fraction of the fluid phase ($F = 0.44$–$0.49$).

The most likely explanation for the shift in the point of connectivity, or percolation threshold, to lower fractions of the fluid phase in the presence of the peptide lies in the effect of the peptide on the shape of the domains. If the shape of the fluid domains becomes more asymmetric (and that of the gel phase domains correspondingly more symmetric) in the presence of the peptide, the point of connectivity will be reduced to lower fractions of the fluid phase. For instance, based on continuum percolation theory, the fluid phase fraction at which disconnection of the fluid phase is achieved would be reduced to the minimum value of 0.33, if the gel phase domains are assumed to be circular in shape above the point of fluid phase connectivity (Almeida et al., 1992). The domain shape is determined to a large extent by the line tension at the domain boundaries, and the corresponding excess free energy per lipid molecule is smaller for larger domains. Because the fluid domains appear to be larger in the presence of the peptide than in its absence (see below), the energetic cost of creating a more asymmetric domain boundary appears not to be as great in the system containing peptide. However, this may not be the only factor contributing to the asymmetry of the domains; most likely the peptide itself also contributes more directly to the domain shape.

## Average number of lipids per fluid domain and average domain density

The average number of spin labels (either lipid or peptide) per disconnected fluid domain, $N_f$, was estimated from $R_f$, which was in turn estimated from $R_{obs}$, as described in Results. This number can be related to the average domain size, i.e., the average number of lipids per fluid domain, $L_f$, as described previously (Sankaram et al., 1992). A distribution of domain sizes is not considered explicitly, so that this quantity must be considered an effective average over all domains. The average density of spin labels in a disconnected fluid domain, $N_f/L_f$, is then given by $cf/F$, where $F$ is the fraction of the total lipids in the fluid state, $f$ is the fraction of spin labels in the fluid phase, and $c$ is the mole fraction of the spin label relative to total lipid. The number of spin labels per fluid domain, normalized to the total mole fraction of spin labels in the fluid phase, therefore, is given by

$$\frac{N_f}{cf} = \frac{L_f}{F}, \qquad (3)$$

where the quantity on the right is related directly to the density of disconnected fluid domains. Consider a total number of, say, $N_T$ lipids: the corresponding number of disconnected

fluid domains is $N_T F/L_f$. The total number of lipids corresponding to one fluid domain (i.e., the reciprocal of the domain density), therefore, is given simply by $L_f/F$. Thus, the experimentally determined quantity on the left of Eq. 3 may be used to estimate the density of disconnected fluid domains and, hence, to discuss the variation in the number of domains with the fraction, $F$, of fluid lipid.

The dependence of $N_f/cf$ on $F$ for the spin-labeled phospholipids, 13-DMPCSL and 16-DSPCSL, in mixed DMPC/DSPC dispersions both with and without the unlabeled pOmpA peptide, and for the pOmpA-IASL spin label in DMPC/DSPC dispersions, is given in Fig. 7. The values of $F$ were obtained as described in Sankaram et al. (1992) from the binary phase diagram of DMPC/DSPC mixtures (Knoll et al., 1981), as were those of $f$ for 13-DMPCSL and 16-DSPCSL under the assumption that the spin-labeled lipids reflect faithfully the distribution of the corresponding parent unlabeled lipids (cf. Sankaram et al., 1992). It was assumed that pOmpA and pOmpA-IASL are localized entirely in the fluid phase, i.e., $f = 1$ for the unlabeled and the spin-labeled peptides. It is seen immediately from Fig. 7, $A$ and $B$ that $N_f/cf$ and, hence, the effective domain density, remains essentially constant with increasing $F$ for the DMPC/DSPC mixtures in the absence of peptide. Therefore, the present measurements with the spin-labeled DSPC component (16-DSPCSL) are fully consistent with the previous findings with the spin-labeled DMPC component (13-DMPCSL) in that, for DMPC/DSPC mixtures alone, the average number of disconnected fluid domains remains constant and simply the domains essentially grow linearly in size with increasing fraction of fluid lipid, $F$ (Sankaram et al., 1992). The total number of lipids per fluid domain, i.e., the reciprocal of the domain nucleation density, deduced from the data for 16-DSPCSL is $L_1$ ($=L_f/F$) = 826 $\pm$ 18 (Fig. 7 $B$), which is in good agreement with the value of 830 $\pm$ 20 deduced previously from data for 13-DMPCSL, in DMPC/DSPC mixtures alone (Fig. 7 $A$ and Sankaram et al., 1992).

In contrast to the situation in the absence of peptide, it is seen from Fig. 7, $C$ and $D$ that for DMPC/DSPC mixtures in the presence of peptide, the effective density of disconnected fluid domains does not remain constant as the fraction of fluid lipid changes. Because the dependence of $N_f/cf$ on $F$ is similar in this respect for the spin-labeled peptide (Fig. 7 $C$) and the spin-labeled lipids in the presence of unlabeled peptide (Fig. 7 $D$), the differences in the presence and absence of peptide are due to the effect of the peptide on the mechanism of domain growth, and not, for instance, to any assumptions regarding the partitioning of the spin label. It is clear from both Fig. 7, $C$ and $D$ that, at low fractions of fluid lipid, $N_f/cf$ is larger (which means that the domain density is lower, and the domains effectively are larger) in the presence of peptide than in the absence of peptide. As $F$ increases so does the domain density until, at values of $F$ close to one, the estimates of the domain density and the domain size in the presence of peptide are comparable to those in the absence of peptide. The implications of this are clear. Because the
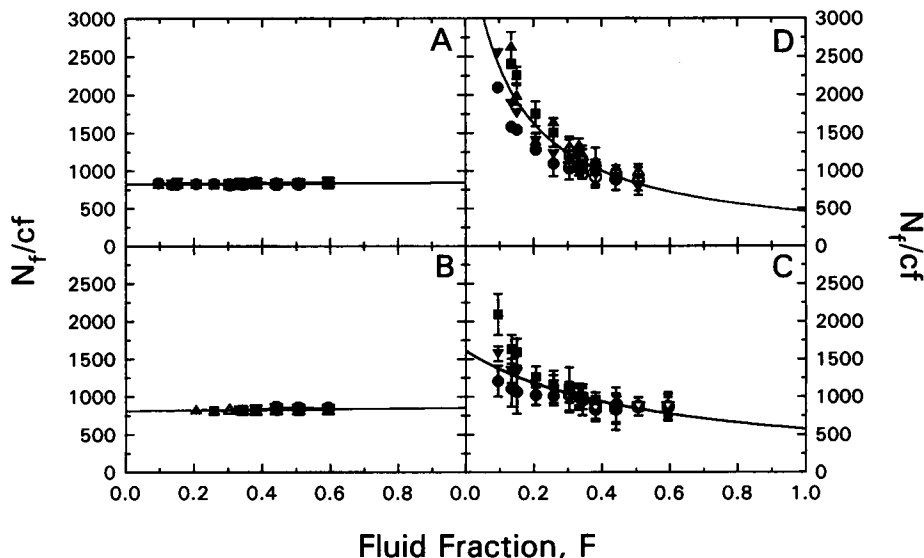
FIGURE 7    Dependence on fluid fraction, $F$, of the average number of spin labels per disconnected fluid domain, $N_f$, normalized for the spin label concentration in the fluid phase, $N_f/c_f$. In panels A–D, the open symbols correspond to data obtained from 50:50 (mol/mol) DMPC/DSPC mixtures and the closed symbols correspond to 40:60 (mol/mol) DMPC/DSPC mixtures. Lines drawn through the points are the result of nonlinear least-squares fit of the data to Eq. 8. (A) 13-DMPCSL in DMPC/DSPC mixtures. The data published in Sankaram et al. (1992) are replotted in this panel. The concentrations of 13-DMPCSL were 2 mol% (O, ●), 2.5 mol% (∇, ▼), 3 mol% (□, ■), and 3.5 mol% (△, ▲) (B) 16-DSPCSL in DMPC/DSPC mixtures. The concentrations of the spin-labeled lipid, 16-DSPCSL, were 1.5 mol% (O, ●), 2 mol% (∇, ▼), 3 mol% (□, ■), and 4 mol% (△, ▲). (C) The peptide spin label, pOmpA-IASL, in DMPC/DSPC mixtures. The concentrations of pOmpA-IASL, were 1 mol% (O, ●), 1.5 mol% (∇, ▼), and 2 mol% (□, ■). (D) The phospholipid spin labels, 13-DMPCSL and 16-DSPCSL, in DMPC/DSPC mixtures containing the unlabeled peptide, pOmpA, at a concentration of 2 mol%. The concentrations of 13-DMPCSL, were 1 mol% (O, ●), 1.5 mol% (∇, ▼), and 2 mol% (□, ■). The concentration of 16-DSPCSL was 2 mol% (△, ▲).

disconnected fluid domains in the presence of peptide initially are larger (and fewer) than are those in the absence of peptide, as the domains grow in size essentially they break up to produce progressively larger numbers of domains. It seems likely that these qualitative conclusions, which are inherent in the primary data (viz. lower values and a steeper drop of $R_{obs}$ for the peptide-containing samples) and are obtained consistently for different spin labels, are independent of any uncertainties in the absolute values of the domain sizes that might arise from limitations in the spectral analysis. To interpret this behavior in the presence of peptide, a model is required for the process of domain fission/coalescence. A simplified model that is consistent with these features of the experimental data is presented in the following section.

## Model for fission/coalescence of disconnected domains

It is assumed that the domains originally formed grow linearly with $F$, as is the case in the absence of peptide, i.e., the number of lipids per disconnected fluid domain is $L_1F$, where $1/L_1$ is the initial nucleation density. However, with increasing $F$ the domains split up to produce fissioned domains of size $z'L_1F$, where $z' < 1$ (in the case of coalescence $z' > 1$). Consider a total of $N_T$ lipids, the total number of lipids in the fluid state is then given by

$$N_T F = nL_1F + n_c z'L_1F, \tag{4}$$

where $n$ is the number of untransformed domains and $n_c$ is

the number that has been produced by fission. For simplicity, it is assumed that the yield of domain fission is proportional to the domain size, $L_1F$, i.e.,

$$\frac{n_c}{N_T} = kL_1F, \tag{5}$$

where $k$ is a constant. This implies that the total number of domains increases linearly with $F$. The average number of lipids per disconnected fluid domain, $L_f$, is simply the total number of fluid lipids divided by the total number of domains, i.e.,

$$L_f = \frac{N_T F}{n + n_c}. \tag{6}$$

Combining Eqs. 4–6 then leads to the following expression for the dependence of the domain size on $F$:

$$L_f = \frac{F}{[kL_1(1 - z')F + 1/L_1]}, \tag{7}$$

and from Eq. 3, the number of spin labels per fluid domain, normalized to the average spin label concentration in the fluid phase, is given by

$$\frac{N_f}{cf} = \frac{1}{[kL_1(1 - z')F + 1/L_1]}. \tag{8}$$

For $z' < 1$ and $k > 0$, this equation predicts that $N_f/cf$ will decrease progressively with increasing $F$ in a pseudo-hyperbolic fashion, and that for $k = 0$ will have a constant

value of $N_f/cf = L_1$. These two cases correspond to the situations in the presence and absence of peptide, respectively.

Nonlinear least-squares fits of Eq. 8 to the data for the pOmpA-IASL and lipid spin labels are given in Fig. 7, $C$ and $D$, respectively. It is seen that this phenomenological model for the domain fission is capable of fitting the data to a reasonable degree of approximation. The values of $L_1$, corresponding to the initial number of total lipids per domain at $F = 0$, determined from the fit are $1610 \pm 105$ and $4390 \pm 730$ for pOmpA-IASL and for the lipid spin labels in the presence of pOmpA, respectively. The difference between these two values may reflect the difficulty in obtaining experimental points at low values of $F$ and uncertainties arising from the spectral analysis (possibly residual spectral anisotropy for the lipid labels), but both are much larger than the corresponding (constant) values obtained in the absence of peptide. The values of $1/[kL_1(1 - z') + 1/L_1]$, corresponding to the limiting number of total lipids per domain extrapolated to $F = 1$, determined also from the fits are: $460 \pm 110$ and $570 \pm 30$, for pOmpA-IASL and for the lipid spin labels in the presence of pOmpA, respectively. These limiting values are much closer to those obtained in the absence of peptide than are the initial values at $F = 0$. It is these aspects of the results that the next section attempts to interpret.

## Physical basis of fluid domain fission/coalescence

One of the most significant effects of the pOmpA peptide on the formation of fluid domains is the increase in effective fluid domain size relative to that found for the natural state of the lipid mixture in the absence of peptide. The origin of this can probably be found in a strong tendency of the peptide to partition into the fluid domains as soon as they are formed. So that the peptide concentration in the fluid domains is not impossibly high when they are formed initially, the domains must be larger, i.e., the domain density lower, than in the natural state. The lipid/peptide ratio in the fluid domains is given by $F/c$, assuming that $f = 1$ for the peptide. Therefore, for peptide concentrations, $c$, up to 2 mol%, the number of lipids per peptide in each domain is $\geq 5$ at the lowest fraction of fluid lipid measured, i.e., $F = 0.1$. This value is not unreasonable because the maximum number of lipids that can be accommodated around a hydrophobic $\alpha$-helix is approximately 10, assuming that it penetrates completely across the membrane (Marsh, 1993). Therefore, it seems quite plausible that the mechanism of domain enlargement at low fluid fractions is the necessity to accommodate all of the peptide in the fluid domains.

At somewhat higher values of $F$, another aspect of the concentration of peptide in the domains may contribute to the domain enlargement. This is the increase in size of the domain perimeter resulting from accommodation of the peptide within the domain. If, as indicated by the experimental data, the fluid fraction essentially is unchanged by introduction of the peptide, the corresponding increase in excess free energy of the gel-fluid interface can be alleviated by reducing the

relative size of the domain boundary. This could be accomplished by the change to a less asymmetric shape (as suggested by the shift in the percolation threshold on addition of peptide; see Table 1) that would result from an increase in domain size accompanying a decrease in the number of disconnected domains relative to that in the absence of peptide.

As the fraction of fluid lipid increases further, the domains grow in size until they no longer suffer the various constraints imposed by a high internal peptide concentration. They are then able to relax to their natural size, i.e., that in the absence of peptide, by domain fission, as is observed. At the highest fractions of fluid lipid for which measurements were made ($F = 0.5$), the value of $L_f/F$ has decreased to 840, which is close to that in the absence of peptide. Under these conditions, the domain density, therefore, has achieved close to its natural state. The driving force for the domain fission is most probably one of entropy of mixing of the domains, and the natural or relaxed state is determined by a balance between this and the line tension at the boundaries of the domains.

As pointed out previously (Sankaram et al., 1992), the domain sizes determined by this method are effective average sizes. Information on the heterogeneity of the size and shape of the domains is not available from these measurements. Preliminary calculations have been performed that were aimed at examining the effect of a possible distribution in domain sizes on the simulated spectra. These showed that, for a Gaussian distribution with a mean number of lipids per disconnected domain of 830 and distribution width of 100 lipids per domain, the dependence of the intensity ratio, $R$, on the mean number of spin labels per domain, $N$, is unchanged relative to that calculated on the assumption of a constant size for all disconnected domains for the range $N > 10$.

The present experiments, therefore, demonstrate a pronounced effect of the peptide on the lipid domain structure. Conversely, an altered domain structure could mediate interactions and properties of a membrane-inserted polypeptide. It is tempting to speculate that lipid domain rearrangements play a role in the in vivo function of signal peptides. For example, when the precursor of an exported protein is delivered to the membrane, the signal peptide may insert into the lipid phase before a proteinaceous translocation complex is recruited. Alterations in the lipid domain structure, mediated by the insertion of the signal peptide, could play a role in favoring the association of the nascent chain with the translocation apparatus. Current results argue strongly that translocation takes place through a largely proteinaceous pore or channel (Simon and Blobel, 1992; Joly and Wickner, 1993; Rapoport, 1992; Crowley et al., 1993). Nonetheless, all of the components exist as membrane proteins whose properties and interactions will be necessarily affected by the physical state of the lipids. Also, biophysical data demonstrate that functional signal peptides share the ability to insert spontaneously into the membrane lipid bilayer (Hoyt and Gierasch, 1991; Killian et al., 1990). Specific roles for signal peptide-lipid interactions have been suggested before (Jones et al., 1990; de Vrije et al., 1988; Batenburg et al., 1988), and our

data point out that these interactions may occur at the level of organization of lipid domains.

A preliminary account of this work has been presented at the 1993 Annual Biophysical Society Meeting (Sankaram et al., 1993).

## REFERENCES

Almeida, P. F. F., W. L. C. Vaz, and T. E. Thompson. 1992. Lateral diffusion and percolation in two-phase, two-component lipid bilayers. Topology of the solid-phase domains in-plane and across the lipid bilayer. *Biochemistry.* 31:7198–7210.

Bales, B. L. 1980. A simple, accurate method of correcting for unresolved hyperfine broadening in the EPR of nitroxide spin probes to determine the intrinsic linewidth and Heisenberg spin exchange frequency. *J. Magn. Res.* 38:193–205.

Bales, B. L. 1982. Correction for inhomogeneous line broadening in spin labels II. *J. Magn. Res.* 48:418–430.

Bales, B. L. 1989. Inhomogeneously broadened spin-label spectra. *In* Biological Magnetic Resonance. Vol. 8. L. J. Berliner and J. Reuben, editors. Plenum Press, New York. 77–130.

Batenburg, A. M., R. A. Demel, A. J. Verkleij, and B. de Kruijff. 1988. Penetration of the signal sequence of *Escherichia coli* PhoE protein into phospholipid model membranes leads to lipid-specific changes in signal peptide structure and alterations in lipid organization. *Biochemistry.* 29: 8229–8240.

Bultmann, T., W. L. C. Vaz, E. C. C. Melo, R. B. Sisk, and T. E. Thompson. 1991. Fluid-phase connectivity and translational diffusion in a eutectic, two-component, two-phase phosphatidylcholine bilayer. *Biochemistry.* 30:5563–5579.

Crowley, K. S., G. D. Reinhardt, and A. E. Johnson. 1993. The signal sequence moves through a ribosomal tunnel into a noncytoplasmic aqueous environment at the ER membrane early in translocation. *Cell.* 73: 1101–1115.

de Vrije, T., R. L. de Swart, W. Dowhan, H. Tommassen and b. de Kruijff. 1988. Phosphatidylglycerol is involved in protein translocation across *Escherichia coli* inner membranes. *Nature.* 334:173–175.

Edidin, M. 1990. Molecular associations and membrane domains. *Curr. Top. Membr. Transp.* 36:81–96.

Eibl, H., and W. E. M. Lands. 1969. A new, sensitive determination of phosphate. *Anal. Biochem.* 30:51–57.

Galla, H.-J., and E. Sackmann. 1975. Chemically induced lipid phase transition in model membranes containing charged lipids: A spin label study. *Biochim. Biophys. Acta* 401:509–529.

Griffith, O. H., and H. M. McConnell. 1966. A nitroxide-maleimide spin label. *Proc. Natl. Acad. Sci. USA.* 55:8–11.

Hoyt, D. W., and L. M. Gierasch. 1991. Hydrophobic content and lipid interactions of wild-type and mutant OmpA signal peptides correlate with their in vivo function. *Biochemistry.* 30:10155–10163.

Joly, J. C., and W. Wickner. 1993. The SecA and SecY subunits of translocase are the nearest neighbors of a translocating preprotein, shielding it from phospholipids. *EMBO J.* 12: 255–263.

Jones, J. D., C. J. McKnight, and L. M. Gierasch. 1990. Biophysical studies of signal peptides: implications for signal sequence functions and the involvement of lipid in protein export. *J. Bioenerg. Biomembr.* 22: 213–232.

Jovin, T. M., and W. L. C. Vaz. 1989. Rotational and translational diffusion in membranes measured by fluorescence and phosphorescence methods. *Methods Enzymol.* 172:471–512.

Killian, J. A., R. C. A. Keller, M. Struyve, A. I. P. M. de Kroon, J. Tommassen, and B. de Kruijff. 1990. Induction of nonbilayer lipid structures by functional signal peptides. *EMBO J.* 9:815–819.

Knoll, W., K. Ibel, and E. Sackmann. 1981. Small-angle neutron scattering study of lipid phase diagrams by the contrast variation method. *Biochemistry.* 20:6379–6383.

Krutzsch, H. C. 1983. Polypeptide sequencing with dipeptidyl peptidases. *Methods Enzymol.* 91:511–524.

Krutzsch, H. C., and J. J. Pisano. 1977. Analysis of dipeptides by gas chromatography-mass spectrometry and application to sequencing with dipeptidyl aminopeptidases. *Methods Enzymol.* 47:391–404.

Lowry, O. H., N. J. Rosebrough, A. C. Farr, and R. J. Randall. 1951. Protein measurement with the Folin phenol reagent. *J. Biol. Chem.* 193:265–275.

Marsh, D., and A. Watts. 1982. Spin labeling and lipid-protein interactions in membranes. In *Lipid-Protein Interactions.* Vol. 2. P. Jost and O. H. Griffith, editors. Wiley-Interscience, New York. 53–126.

Marsh, D. 1993. The nature of the lipid-protein interface and the influence of protein structure on protein-lipid interactions. In *New Comprehensive Biochemistry.* Vol. 25. A. Watts, editor. Elsevier, Amsterdam. 41–66.

Melo, E. C. C., I. M. G. Lourtie, M. B. Sankaram, T. E. Thompson, and W. L. C. Vaz. 1992. Effect of domain connection and disconnection on the yields of in-plane bimolecular reactions in membranes. *Biophys. J.* 63:1506–1512.

Rapoport, T. A. 1992. Transport of proteins across the endoplasmic reticulum membrane. *Science.* 258:931–936.

Sachse, J.-H., M. D. King, and D. Marsh. 1987. ESR determination of lipid translational diffusion coefficients at low spin-label concentrations in biological membranes, using exchange broadening, exchange narrowing, and dipole-dipole interactions. *J. Magn. Res.* 71:385–404.

Sackmann, E., and H. Traeuble. 1972. Studies of the crystalline-liquid crystalline phase transition of lipid model membranes. I. Use of spin labels and optical probes as indicators of the phase transition. *J. Am. Chem. Soc.* 94:4482–4491.

Sackmann, E., and H. Traeuble. 1972. Studies of the crystalline-liquid crystalline phase transition of lipid model membranes. II. Analysis of electron spin resonance spectra of steroid labels incorporated into lipid membranes. *J. Am. Chem. Soc.* 94:4492–4510.

Sankaram, M. B., and T. E. Thompson. 1990. Interaction of cholesterol with glycerophospholipids and sphingomyelin. *Biochemistry.* 29: 10670–10675.

Sankaram, M. B., and T. E. Thompson. 1992. Deuterium magnetic resonance study of phase equilibria and membrane thickness in binary phospholipid mixed bilayers. *Biochemistry.* 31:8258–8268.

Sankaram, M. B., D. Marsh, and T. E. Thompson. 1992. Determination of fluid and gel domain sizes in two-component, two-phase lipid bilayers. An ESR spin label study. *Biophys. J.* 63:340–349.

Sankaram, M. B., L. M. Gierasch, and T. E. Thompson. 1993. Modulation of in-plane lipid domain structure in bilayers by signal peptides. *Biophys. J.* 64:71a. (Abstr.)

Sankaram, M. B., J. D. Jones, and L. M. Gierasch. 1993. Correlation between membrane export of *Escherichia coli* outer membrane protein A and membrane penetration potential of its signal sequences. *Biophys. J.* In press.

Simon, S. M., and G. Blobel. 1992. Signal peptides open protein-conducting channels in *E. coli. Cell* 69:677–684.

Thompson, T. E., M. B. Sankaram, and R. L. Biltonen. 1992. Biological membrane domains: functional significance. *Comments Mol. Cell. Biophys.* 8:1–15.

Vaz, W. L. C., E. C. C. Melo, and T. E. Thompson. 1989. Translational diffusion and fluid domain connectivity in a two-component, two-phase phospholipid bilayer. *Biophys. J.* 56:869–876.

Vaz, W. L. C., E. C. C. Melo, and T. E. Thompson. 1990. Fluid phase connectivity in an isomorphous, two-component, two-phase phosphatidylcholine bilayer. *Biophys. J.* 58:273–275.

Vaz, W. L. C. 1992. Translational diffusion in phase-separated lipid bilayer membranes. *Comments Mol. Cell. Biophys.* 8:17–36.